Article

Transcriptome and Metabolome Analyses of Glucosinolate Biosynthesis-Related Genes in Different Organs of Broccoli (*Brassica oleracea* L. var. *italica*)

Xiuling Tian [1], Hongju He [1], Xiaolu Yu [1], Yaqin Wang [1], Liping Hu [1], Bing Cheng [1], Yunhua Ding [2,*] and Guangmin Liu [1,*]

[1] Institute of Agri-Food Processing and Nutrition, Beijing Academy of Agriculture and Forestry Sciences, Beijing 100097, China; tianxiuling@iapn.org.cn (X.T.); hehongju@iapn.org.cn (H.H.); yuxiaolu@iapn.org.cn (X.Y.); wangyaqin@iapn.org.cn (Y.W.); huliping@iapn.org.cn (L.H.); chengbing@iapn.org.cn (B.C.)

[2] Vegetable Research Center, Beijing Academy of Agriculture and Forestry Sciences, Beijing 100097, China

* Correspondence: dingyunhua@nercv.org (Y.D.); liuguangmin@iapn.org.cn (G.L.)

Abstract: Broccoli (*Brassica oleracea* L. var. *italica*) is a globally popular vegetable because of its nutrient richness, especially its glucosinolates (GSLs). The content of GSLs in different organs of broccoli varies greatly. However, few studies have focused on the differences in the GSLs biosynthesis-related genes in different organs. In this study, we selected extreme individuals from an F_2 population of broccoli and mixed them to form low and high glucoraphanin content pools of leaf, stalk and floret, respectively. Transcriptome and metabolome analyses showed that 539, 755 and 617 genes are significantly differentially expressed, and 44, 66 and 118 metabolites are significantly differentially accumulated in leaf, stalk and floret comparison groups, respectively. The combined analysis revealed that some genes such as *Bo5g113720*, *Bo2g161100* and *Bo7g09800*, *Bo4g018590*, *Bo5g021810*, and *Bo2g011730* showed different expression trends between low and high glucoraphanin content pools, which increased the accumulation of glucoraphanin. These genes have different expression levels in the three plant parts. Strikingly, the accumulation of glucoraphanin upregulated the expression of plant hormone signal transduction-related genes *TIFY*, *JAR1*, *IAA*, *GH3* and *SAU*, and also increased the levels of tentatively identified flavonoid metabolites. Our study deepens the understanding of glucosinolate biosynthesis in different organs at the molecular level, and also provides evidence for the crosstalk between glucosinolates and flavonoids biosynthesis pathways.

Keywords: broccoli; glucosinolates; flavonoid; transcriptome; metabolome

1. Introduction

Broccoli (*Brassica oleracea* L. var. *italica*) is a globally popular vegetable crop of the *Brassicaceae* family that contains several nutrients like glucosinolates (GSLs) and other biologically active compounds [1,2]. GSLs are secondary metabolites, which play an essential role in the anti-insect, anti-pathogen activities in plants, and which have cancer-preventing properties [3–6]. They are specific functional compounds found in almost exclusively cruciferous plants, including *Brassica* crops such as broccoli, rapeseed, cauliflower and the model plant *Arabidopsis thaliana* [7,8]. Previous studies have shown that broccoli is rich in GSLs, especially 4-(methylsulfinyl)butyl (glucoraphanin, RAA) and indol-3-methyl (glucobrassicin, GBC) glucosinolate, which are beneficial to human health [9–11].

In broccoli, it has been reported that the major GSL, i.e., glucoraphanin (RAA), is the precursor to sulforaphane [12]. As soon as broccoli tissues are damaged, glucoraphanin is hydrolyzed by myrosinase into an isothiocyanate, namely sulforaphane [13,14]. Sulforaphane is a natural plant compound with antioxidant and antimicrobial properties. Some

studies have reported that sulforaphane could effectively reduce the development and recurrence of cancer, thereby improving patient survival [15,16]. Furthermore, sulforaphane can protect against heart disease [17].

The GSLs constitute a well-defined group of secondary metabolites with many effects on plant defense, taste and health benefits [18–21]. Although high numbers of natural GSLs have been listed in older papers, a recent critical revision concluded that the number of scientifically validated GSLs is less than 100 [18]. GSLs can be divided into three types according to their variable side chain structure, i.e., aliphatic GSLs derived from alanine, leucine, isoleucine, valine or methionine, benzenic GSLs derived from phenylalanine or tyrosine, and indolic GSLs derived from tryptophan [18–21]. GSLs biosynthesis proceeds in three stages; firstly, the side chains of respective precursor amino acids were elongated; secondly, the formation of core structures of GSLs; and thirdly, secondary modifications of amino acid side chains by methoxylation, desaturation, hydroxylation, oxidation or benzoylation [5,22].

GSLs levels in broccoli are determined by genotypes, as well as by genotype-environment interactions [23]. Moreover, many factors also significantly affect GSLs content in broccoli during growing seasons, including organ, developmental phase, cultivation and climate conditions [24,25]. The genes related to the biosynthesis of GSLs mainly involve three biosynthetic steps and some regulatory genes. Most of them have been discovered, identified and functionally validated in *Arabidopsis thaliana* [22,26,27]. The aliphatic GSLs biosynthesis pathway depends upon *BCAT* and *MAM* for deamination and the process of chain elongation [28]. The formation of the core structure involves multiple biochemical reaction processes, in which cytochrome the P450 *CYP79* and *CYP83* gene family, C-S lyase *SUR1*, the *UGT74* gene family, and sulfotransferases *SOT16/17/18* play essential roles in these processes [5,29]. Secondary modifications of the side chain have been regulated by *FMOGS-OX1-5*, *APO2*, *APO3* and *GS-OH* [5]. Moreover, the transcription factor *MYB* gene family plays a crucial role in regulating the above GSLs biosynthesis genes [30]. Previous studies have primarily focused on the effect of external conditions on GSLs content, while there is little evidence of the effects of genotype and developmental organs in broccoli.

The objective of this study was to explore the differences in GSLs biosynthesis-related genes in different organs. Here, we formed contrasting bulk segregant populations of leaf, stalk and floret based on the glucoraphanin content from an F_2 broccoli population. The gene expression and metabolomics between low and high glucoraphanin content pools of three organs were compared by integrated transcriptome and metabolome analysis. In addition, we found that the accumulation of glucoraphanin affects the levels of flavonoid metabolites. These results deepen the understanding of GSLs biosynthesis in different parts at the molecular level, and also provide evidence for the crosstalk between GSLs and flavonoid biosynthesis pathways.

2. Materials and Methods

2.1. Plant Materials and Growth Conditions

An F_2 broccoli population containing 500 individuals obtained from a cross between the inbred lines B0401 and MS84003 was used for transcriptome sequencing and metabolome analysis. F_2 plants and the parental lines were planted in the greenhouse at the vegetable research center, Beijing Academy of Agriculture and Forestry Sciences during the 2021–2022 growing season. The parental lines B0401 and MS84003 had a significant difference in glucoraphanin content.

2.2. Extraction and Determination of Glucosinolates

In total, 400 F_2 individual plants were sampled. From half of them (200 plants), the stalk and all leaves at the vegetative growth stage were taken and quickly frozen in liquid nitrogen, and stored at −80 °C conditions. The other half (200 plants) were grown to the stage suitable for the commercial harvest of heads. Half of the heads were dried by vacuum freeze drying, and the other half were stored at −80 °C conditions. Sample powders were

weighted 0.5 g (freeze-dried) or 0.1 g (fresh) for extraction, and they were extracted using 70% (freeze-dried sample) or 80% methanol (fresh sample). The detailed extraction and determination methods of glucosinolates were according to the previous reports from our lab [31].

2.3. Forming the Bulks Segregant Pools

According to the glucoraphanin content in the three parts of F_2 individual plants, extreme individuals were selected and their fresh powder of the same weight were thoroughly mixed to form the high and low glucoraphanin content pools of stalk, leaf and floret, respectively. Each pool contained 25 individual plants. For each plant part, the same extreme pool was used for transcriptome and metabolome analysis. To make it easier to distinguish transcriptome and metabolome, we named LTL (leaf), STL (stalk), and FTL (floret) for the low glucoraphanin content pools used for transcriptome; and named LTH (leaf), STH (stalk), and FTH (floret) for the high glucoraphanin content pools used for transcriptome. Meanwhile, we named LML (leaf), SML (stalk), and FML (floret) for the low glucoraphanin content pools used for metabolome; and named LMH (leaf), SMH (stalk), and FMH (floret) for the high glucoraphanin content pools used for metabolome. For data reliability, each pool had three biological replicates, denoted by the suffixes 1, 2, and 3, such as the three biological repeats of LTL named LTL1, LTL2, and LTL3.

2.4. RNA-Seq and Quantitative PCR (qPCR) Expression Analysis

Three biological replicates of stalk and leaf at the vegetative growth stage, and floret at the commercial stage, were collected from high and low glucoraphanin content pools, respectively. RNA extraction and sequencing were performed by Metware Biotechnology Co., Ltd. (Wuhan, China). Approximately six Gb of transcriptomic data for each segregant pool was available through the Illumina sequencing platform. Clean reads were obtained by filtering low-quality reads from raw reads and then mapped to the *Brassica oleracea* reference genome. The differentially expressed genes (DEGs) were identified on the basis of |Fold Change| > 2 and $p < 0.05$. The significant enrichment threshold for the Kyoto Encyclopedia of Genes and Genomes (KEGG) pathway analysis was p-value < 0.05. The gene functional annotation was aligned with the related species to create a predicted protein interaction network.

Fresh stalk and leaf at the vegetative growth stage and floret at the commercial stage were collected for qPCR assays. Total RNA was extracted from frozen samples using EasyPure Plant RNA Kit (ER301, Transgene, Beijing, China). Reverse transcription was performed using an ABScript III RT Master Mix for qPCR kit with gDNA Remover (RK20429, ABclonal, Wuhan, China). The qRT-PCR analyses were performed using a 2 × Universal SYBR Green Fast qPCRMix (RK21203, ABclonal, Wuhan) kit in a BioRad CFX system following the instructions of the manufacturer. Three biological replicates were performed for each sample. The primer pairs used for qRT-PCR were designed using DNAMAN software. The *Actin* gene was selected as an internal control. The relative quantification gene expression level was calculated by the $2^{-\Delta\Delta Ct}$ method [32].

2.5. Metabolomics Analysis

Metabolomics analysis was performed on 1 g flash-frozen powder of high and low glucoraphanin pools of stalk, leaf at the vegetative growth stage, and floret at commercial harvest stage. Three replicates were performed for each group. The metabolomics analysis was performed by Metware Biotechnology Co., Ltd. (Wuhan, China) using standard procedures. Each sample was represented by three biological replicates. The UPLC-MS/MS system, equipped with an ESI Turbo Ion-Spray interface, operated in positive and negative ion modes, were used for data acquisition. LIT and triple quadrupole (QQQ) scans were performed on a triple quadrupole-linear ion trap mass spectrometer (QTRAP).

According to the secondary spectrum information, the metabolites were qualitatively analyzed by the self-built database of Metware. The changes in metabolites between groups

were represented by principal component analysis (PCA) and orthogonal partial least-squares-discriminant analysis (OPLS-DA). Significantly regulated metabolites between groups were identified by VIP > 1 and |Fold Change| > 2. The metabolites were annotated by the KEGG compound database (http://www.kegg.jp/kegg/compound/, accessed on 20 July 2022), and then mapped to the KEGG pathway database (http://www.kegg.jp/kegg/pathway.html, accessed on 22 July 2022).

2.6. Correlation Analysis of the Transcriptome and Metabolome Data

The DEGs and DAMs were mapped to the KEGG pathway database based on the transcriptome and metabolome data to obtain the common pathway. The correlation between DEGs and DAMs was identified on the basis of Pearson's correlation coefficient (PCC) values > 0.8 and $p < 0.05$, and shown by a nine-quadrant plot. Cytoscape software was used to make connection network graphs between DEGs and DAMs (http://cytoscape.org/, accessed on 15 August 2022).

2.7. Statistical Analyses

All data were analyzed by SAS 9.4 based on $p < 0.05$ for declaration of significance (https://www.sas.com, accessed on 20 August 2022). Gene expression analysis was performed using GraphPad Prism 8 (https://www.graphpad.com/, accessed on 20 August 2022). Principal component analysis (PCA) and orthogonal partial least-squares-discriminant analysis (OPLS-DA) were used SIMCA software v14.1© (Umetrics AB, Malmo, Sweden).

3. Results

3.1. Bulked Segregant Pools Construction

Six types of GSLs were mainly detected in the parental lines B0401 and MS84003, with a significant difference in glucoraphanin RAA (2.38 umol/g DW, 7.91 umol/g DW, respectively) ($p < 0.01$) (Figure S1A, Table S1). Four hundred F_2 plants were selected to determine the GSLs content of leaf and stalk at the vegetative growth stage and floret at the commercial stage, respectively (Figure S1B–D). According to the glucoraphanin (RAA) content, we mixed extreme individuals to form high and low-bulked segregant pools, which consisted of 25 individual plants per pool.

3.2. RNA-Seq, Assembly, and Functional Annotation

In total, three pairs of cDNA libraries were constructed from broccoli leaf (LTL vs. LTH), stalk (STL vs. STH) and floret (FTL vs. FTH) (Table S2). Transcriptome sequencing was performed on the Illumina HiSeq 4000 platform to determine changes in gene expression in the different plant parts. Through quality assessment and low-quality data screening, 41,924,478–66,898,954 high-quality reads were obtained with Q30 > 91.8%, Q20 > 97.1% and average GC content of 47.1% (Table S2); whereas more than 84.8% of reads were uniquely mapped, indicating the selected reference genome (https://plants.ensembl.org/Brassica_oleracea/Info/Index, accessed on 5 July 2022) was appropriate (Table S2). Moreover, a total of 29,010–31,880 unigenes were also assembled and annotated by KEGG, Swiss-Prot, GO, Pfam, NR, and EuKaryotic Orthologous Groups (KOG) databases (Figure S2, Table S3).

3.3. DEGs Identification, GO Enrichment, and KEGG Pathway Analysis

The number of expressed genes in the three pairs (LTL vs. LTH, STL vs. STH, FTL vs. FTH) is shown in Table S3. Fragments per kilobase of transcript per million mapped reads (FPKM) values were used to represent gene expression level, and |Fold Change| > 2 and $p < 0.05$ were used as thresholds for significant differentially expressed genes (DEGs) selection. The results showed that there were 539 (203 upregulated, 336 downregulated), 755 (402 upregulated, 353 downregulated), and 617 (308 upregulated, 309 downregulated) DEGs obtained in the low and high RAA content pools of the leaf, stalk and floret, respectively (Figure 1A, Table S3). The hierarchical clustering of the three plant parts of DEGs

is shown in Figure 1B. Subsequently, twenty DEGs were also identified in the three plant parts simultaneously (Figure 1C, Table S4).
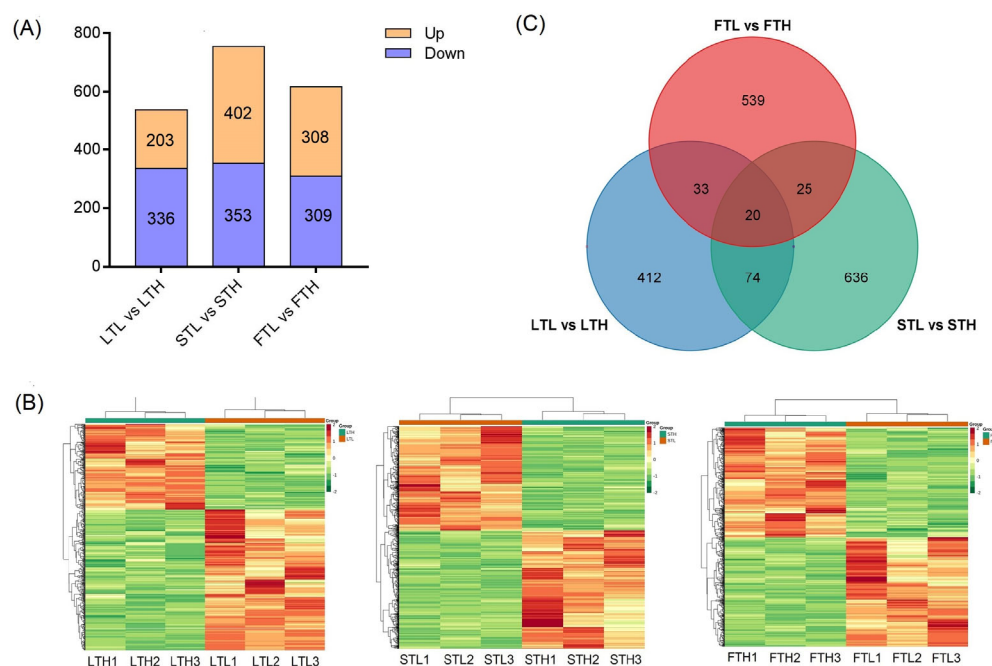

Figure 1. Changes in DEGs expression. (**A**) Upregulation and downregulation of DEGs in LTL vs. LTH, STL vs. STH, and FTL vs. FTH. The yellow box represents upregulation, and the blue box represents downregulation. (**B**) Heatmaps of DEGs compared between different groups. (**C**) Coregulation of DEGs in all comparison groups. LTL (LTL1, LTL2, LTL3), STL (STL1, STL2, STL3) and FTL (FTL1, FTL2, FTL3) represent low RAA content pools in leaf, stalk and floret, respectively. LTH (LTH1, LTH2, LTH3), STH (STH1, STH2, STH3) and FTH (FTH1, FTH2, FTH3) represent high RAA content pools in leaf, stalk and floret, respectively.

To better understand the biological functions of DEGs identified between the low and high RAA content pools in three plant parts, GO enrichment analysis was used for functional classification. The result showed that DEGs classified in ontological biological processes (BPs), cellular components (CCs), and molecular functions (MFs) were obtained for the three comparison groups (Figure S3). Among the DEGs of leaf, the upregulated DEGs were mainly involved in the glucosinolate metabolic process, S-glycoside metabolic process (BPs), oxidoreductase activity (MFs), and secretory vesicle (CCs) (Table S5). In the stalk, the main GO terms of upregulated DEGs were the circadian rhythm (BPs), cysteine-type endopeptidase inhibitor activity (MFs), and secretory vesicle (CCs) (Table S5). In the floret, the main GO terms of upregulated DEGs were glucosinolate metabolic process and glucosinolate biosynthetic process (BPs), sugar transmembrane transporter activity and carbohydrate transmembrane transporter activity (MFs), and the monolayer-surrounded lipid storage body (CCs) (Table S5). The above results indicated that it had homogeneity in the DEGs among different plant parts pools.

To further investigate the potential functions of those DEGs between the low and high RAA content pools of three plant parts, KEGG pathway enrichment analyses were performed on DEGs, respectively. The top 10 enrichment pathways are visualized in Figure 2A–C. It showed that "glucosinolate biosynthesis" and "biosynthesis of secondary metabolites" were found to be significantly enriched in the three plant parts pools (Figure 2A–C); "plant hormone signal transduction", "alpha-Linolenic acid metabolism", "linoleic acid metabolism", and "caffeine metabolism" were found to be significantly enriched in leaf and stalk pools (Figure 2A,B); whereas "2-oxocarboxylic acid metabolism" was significantly enriched in the leaf and floret pools (Figure 2A,C). These results indicated that the different organs of

broccoli undertook active metabolic and genetic processes, and the enrichment analyses of the KEGG pathway provided a valuable resource for studying specific pathways and processes in broccoli.
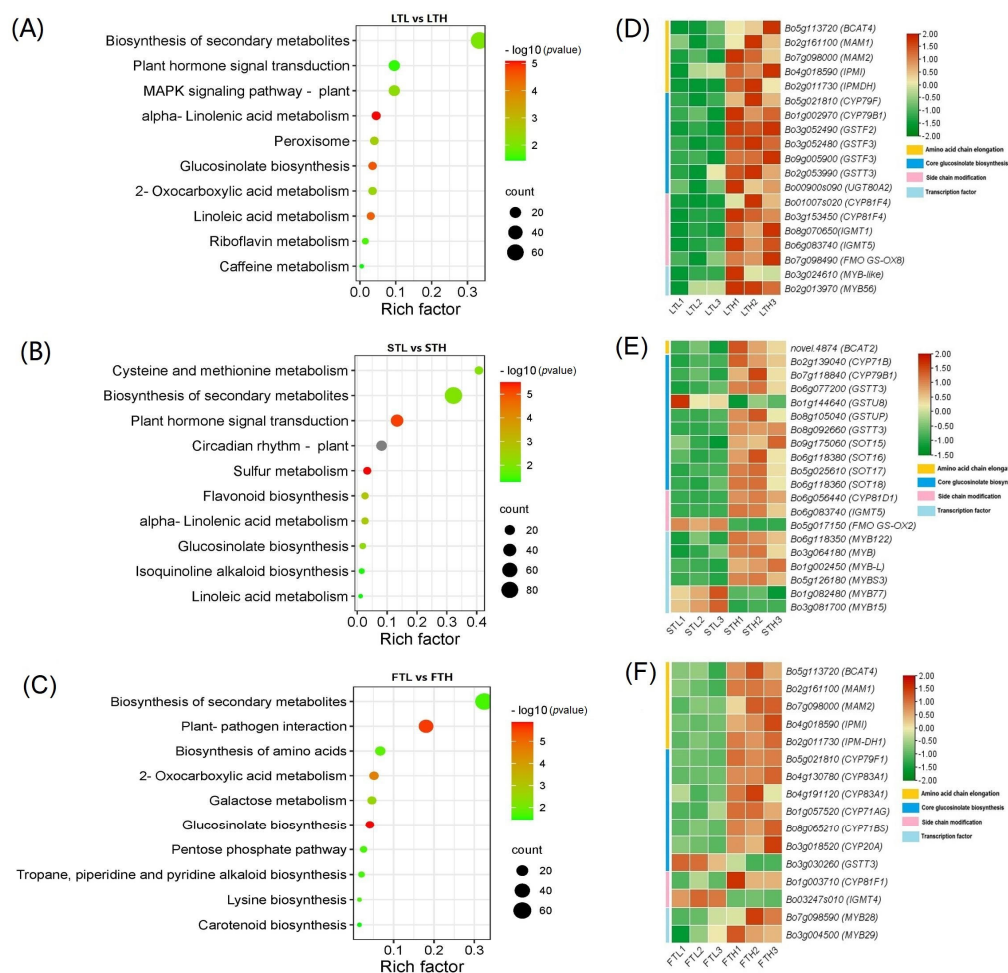

Figure 2. KEGG pathway enrichment analyses of DEGs identified between low and high RAA content pools. The top 10 KEGG pathways of significance of the upregulated and downregulated DEGs in LTL vs. LTH (**A**), STL vs. STH (**B**), and FTL vs. FTH (**C**). The X−axis represents the rich factor; the Y−axis represents the name of the pathway. The bubbles color indicate the enrichment degree of pathway and the size represents the number of DEGs enrichment in the pathway. DEGs related to glucosinolate biosynthesis in leaf (**D**), stalk (**E**), and floret (**F**) between low and high RAA content pools. LTL, STL and FTL represent low RAA content pools in leaf, stalk and floret, respectively. LTH, STH and FTH represent high RAA content pools in leaf, stalk and floret, respectively.

3.4. Identification of DEGs Related to Glucosinolate Biosynthesis

We further investigated the DEGs related to glucosinolate biosynthesis and found that 17, 14 and 14 DEGs were involved in glucosinolate biosynthesis in the three plant parts, respectively (Figure 2D–F, Table S6). Among them, compared to low RAA content pools, all 17 DEGs were upregulated in the high RAA content pool of leaf (Figure 2D, Table S5). While 12 of 14 DEGs were upregulated in the high RAA content pool of stalk and floret, respectively (Figure 2E,F, Table S6). As an essential transcription factor, *MYB* plays a critical regulatory role in glucosinolate biosynthesis. In this study, 98, 110, and 136 *MYB* were found in leaf, stalk and floret, and 2, 6, and 2 had a significantly difference, respectively (Figure 2D–F, Table S6).

Strikingly, six genes (*Bo5g113720*, *Bo2g011730*, *Bo2g161100*, *Bo7g098000*, *Bo4g018590*, *Bo5g021810*) were differentially expressed between the low and high RAA content pools in

leaf and floret (Figure 2D,F, Table S6). *Bo6g083740* was differentially expressed between low and high RAA content pools in leaf and stalk (Figure 2D,E, Table S6). Phylogenetic analysis showed that *Bo5g113720* had high similarity with *BCAT4* of *Arabidopsis thaliana*, which encodes a methionine-oxo-acid transaminase and is involved in the methionine chain elongation pathway that leads to the ultimate biosynthesis of methionine-derived GSLs (Figure S4A). *Bo2g161100* and *Bo7g098000* had high similarity with *MAM1* of Brassica rapa, and it catalyzed the aliphatic GSLs synthesis with short-chain (Figure S4C). *Bo5g021810* showed high similarity with *CYP79F1* of *Brassica rapa* and *Arabidopsis thaliana* (Figure S4E), and it played a critical role in the formation of the core structure 6. Meanwhile, *Bo2g011730* and *Bo4g018590* were similar to *UNE12* and *IPMI2* of *Arabidopsis thaliana* (Figure S4B,D). The results of RNA-Seq and qRT-PCR analysis all showed that all these genes were upregulated in the high RAA content pools compared to the low pools (Figure 3A, Table S7). In addition, we also selected six DEGs related GSLs biosynthesis to verify the results of RNA-seq gene expression in the stalk, and qRT-PCR analysis was well matched with RNA-seq analysis (Figure 3B, Table S7).
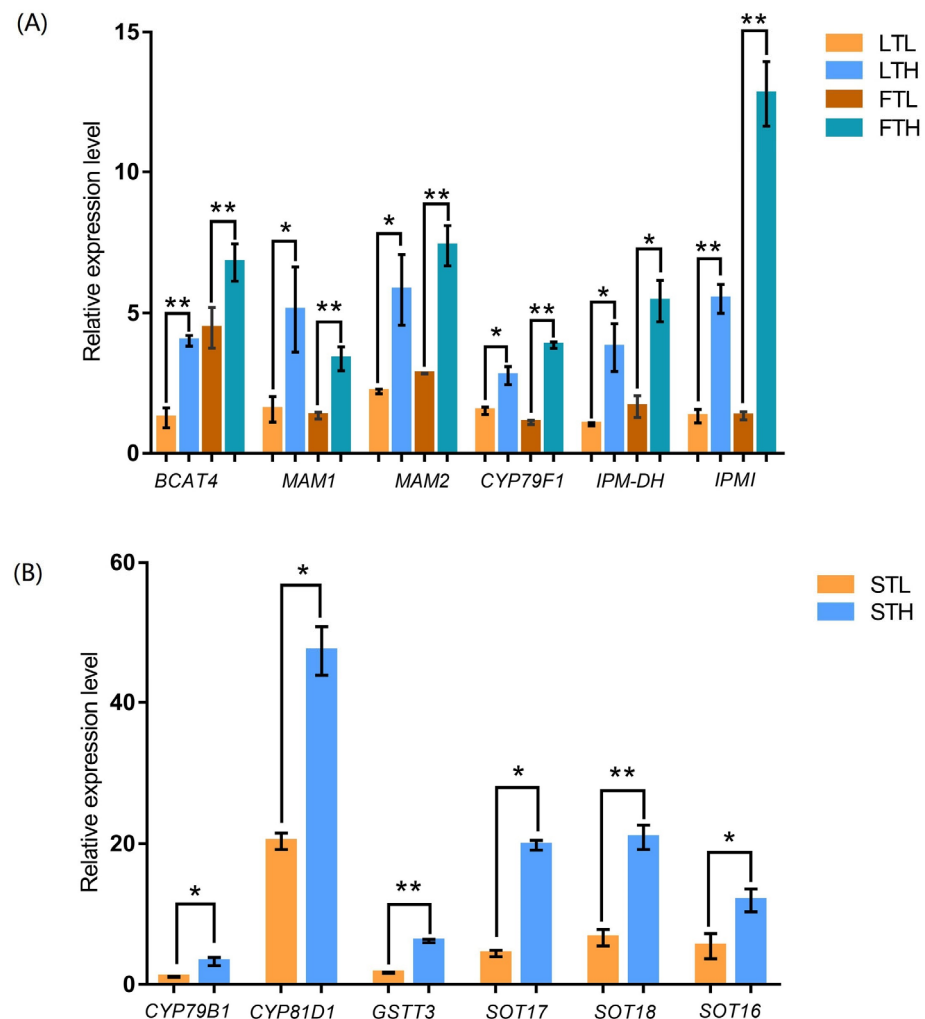

Figure 3. The relative expression level of DEGs related to glucosinolate biosynthesis in leaf, floret (**A**) and stalk (**B**). The error bars represent the SD from three replicates. LTL, STL and FTL represent low RAA content pools in leaf, stalk and floret, respectively. LTH, STH and FTH represent high RAA content pools in leaf, stalk and floret, respectively. * $p < 0.05$, ** $p < 0.01$.

*3.5. Metabolomic Analysis between Low and High RAA Content Pools*

In this study, we performed a widely targeted metabolomic using UPLC-MS/MS in three pairs from the leaf (LML vs. LMH), stalk (SML vs. SMH) and floret (FML vs. FMH)

of broccoli, respectively. The metabolic profile showed that 757, 734 and 1002 metabolites were identified in the leaf, stalk and floret, respectively. Orthogonal partial least squares discrimination analysis (OPLS-DA) was subsequently performed, and the score showed that low and high RAA content pools displayed significant segregation in the three plant parts, respectively (Figure 4A–C). Moreover, PC1 explained more than 45% of the variability in the three plant parts (Figure S5A–C). The metabolite content was normalized to construct a hierarchical clustering heatmap (Figure 4D).
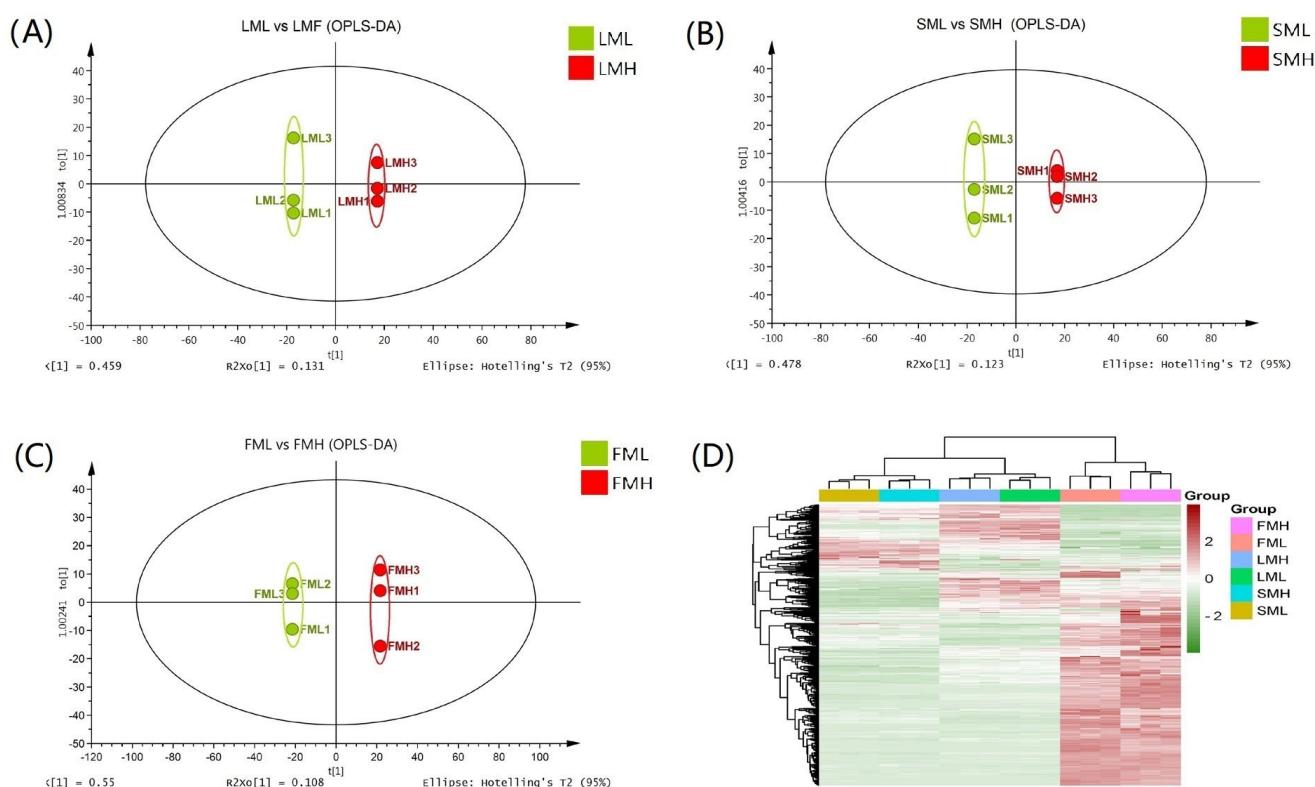
Figure 4. Metabolomics profiling between low and high RAA content pools. Orthogonal partial least squares-discriminant analysis (OPLS−DA) in LML vs. LMH (**A**), SML vs. SMH (**B**), and FML vs. FMH (**C**). (**D**) Heatmap based on hierarchical clustering analysis. LML, SML and FML represent low RAA content pools in leaf, stalk and floret, respectively. LMH, SMH and FMH represent high RAA content pools in leaf, stalk and floret, respectively.

The identification of DAMs in each comparison group (LML vs. LMH, SML vs. SMH, FML vs. FMH) was mainly based on the variable importance in projection (VIP) > 1 and accumulation fold change > 2 or <0.5. Among these detected metabolites, 44 (14 upregulated, 30 downregulated), 66 (33 upregulated, 33 downregulated) and 118 (89 upregulated, 29 downregulated) metabolites underwent significant changes in LML vs. LMH, SML vs. SMH and FML vs. FMH, respectively (Figure 5A, Table S3). The heatmap of DAMs showed that the accumulated metabolites mainly concentrated in ten categories of substances in all the groups (Figure 5B–D, Table S8). Based on conjoint analysis, the common accumulation of three metabolites changed in each group; stalk and floret groups had changed nine common accumulation metabolites, leaf and stalk groups had changed eight common accumulation metabolites, while leaf and floret groups also had changed eight common accumulation metabolites (Figure S6, Table S9).
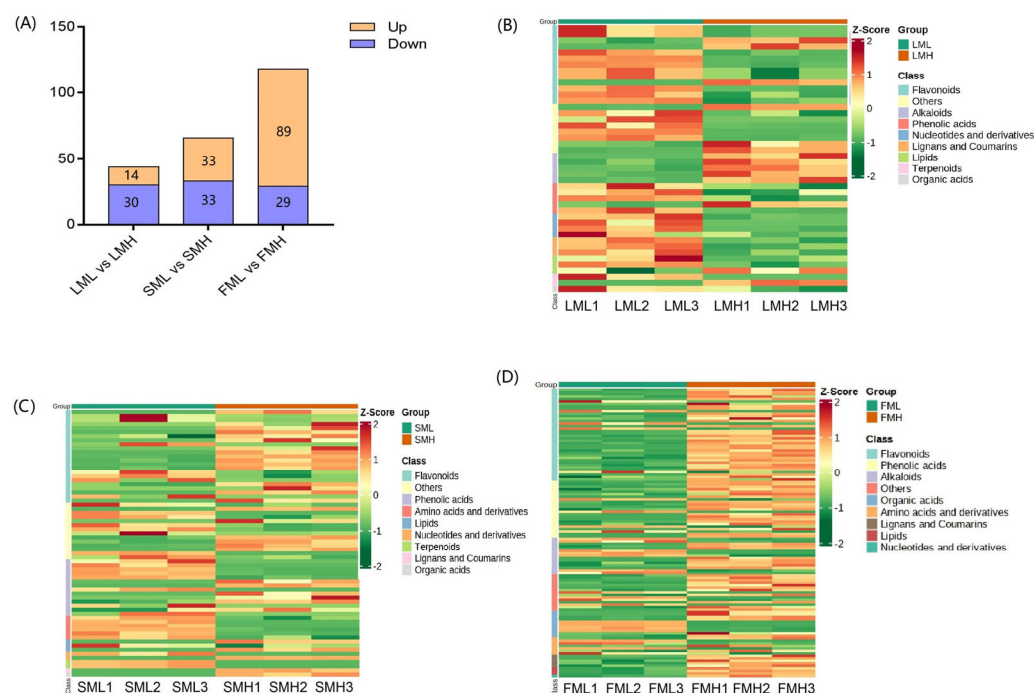
Figure 5. Differential metabolites analysis. (**A**) Upregulation and downregulation of DAMs between different groups. The yellow box represents upregulation, and the blue box represents downregulation. Heatmap of DAMs between LML and LMH (**B**), SML and SMH (**C**), FML and FMH (**D**). LML (LML1, LML2, LML3), SML (SML1, SML2, SML3) and FML (FML1, FML2, FML3) represent low RAA content pools in leaf, stalk and floret, respectively. LMH (LMH1, LMH2, LMH3), SMH (SMH1, SMH2, SMH3) and FMH (FMH1, FMH2, FMH3) represent high RAA content pools in leaf, stalk and floret, respectively. The different colors on $Y-$axis of (**B–D**) represent different metabolite categories.

3.6. KEGG Analysis of Differential Metabolites

To characterize the complex biological behaviors of metabolites that interact in organisms, we annotated the DAMs using the KEGG database. In the leaf group, 36 DAMs were enriched in 21 pathways, 34 DAMs were enriched in 21 pathways for the stalk group, and 85 DAMs were enriched in 34 pathways for the floret group (Figure S7A–C). Among the enrichment pathways of DAMs, flavonoid biosynthesis, biosynthesis of cofactors, biosynthesis of secondary metabolites, ABC transporters, and metabolic pathways were enriched in all three comparison groups. Glucosinolate biosynthesis was enriched in stalk and floret groups. Valine, leucine and isoleucine biosynthesis were only enriched in the floret group (Figure S7A–C). The top 10 significant enrichment pathways in the three comparison groups are shown in Figure S8A–C. The above results were basically consistent with the transcription results.

### 3.7. Joint Analysis of the Transcriptome and Metabolome Data

To further understanding of the pathway of GSLs biosynthesis, we performed a combined transcriptomic and metabolomic analysis for each group. The correlation analysis between DEGs and DAMs showed that many genes were positively correlated with metabolites in the LML vs. LMH, SML vs. SMH, and FML vs. FMH comparisons (Figures 6A and S9A,B). Through KEGG enrichment analysis, we found that many DAMs and DEGs were enriched in the same pathway (Figures 6B and S9C,D). The above results indicated that the accumulation of these metabolites might be regulated by the corresponding genes.
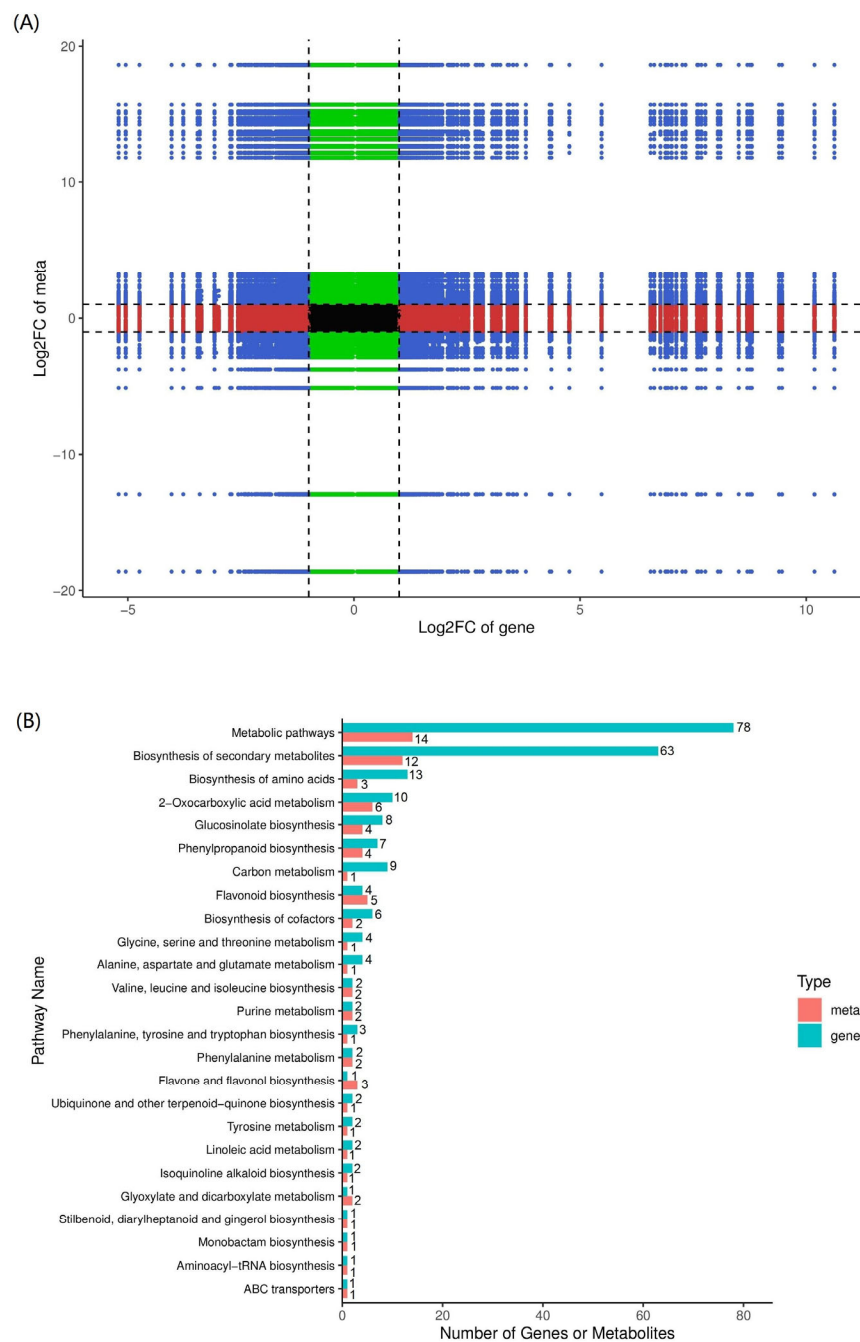
Figure 6. Correlation analyses between transcriptome and metabolome in FML vs. FMH. (**A**) The nine-quadrant diagram shows the correlation of genes and compounds between FML and FMH. (**B**) KEGG enrichment analysis of DEGs (red column) and DAMs (blue column) enriched in the same pathway. FML and FMH represent low and high RAA content pools in floret, respectively.

In the floret comparison group, we found DEGs and DAMs were mainly enriched in 25 pathways, such as the metabolic pathway, biosynthesis of secondary metabolites, 2-Oxocarboxylic acid metabolism, biosynthesis of amino acids, and GSLs biosynthesis (Figure 6B). Glucoraphanin contained significantly different accumulates between FML and FMH. We built a connection network between DEGs and DAMs of glucoraphanin biosynthesis. The result showed that glucoraphanin (MWSmce416) contained a positive correlation with eight genes, which were enriched in the GSLs biosynthesis pathway (Figure 7B). The eight genes also had a positive correlation with benzyl glucosinolate (Cmln001356), 3-Indolylmethyl glucosinolate (Lmyn002727), and a negative correlation

with l-Tyrosine (mws0250) (Figure 7B). In addition, we also built a connection network between DEGs and DAMs of glucoraphanin biosynthesis in the stalk group. The result showed that 13 genes had positive correlations, and one gene (*Bo5g017130*) had a negative correlation with glucoraphanin (MWSmce416) (Figure 7A). The above results indicated that metabolism is a complex biological process. Generally, one metabolite was regulated by multiple genes, or one gene was regulated by different metabolites.
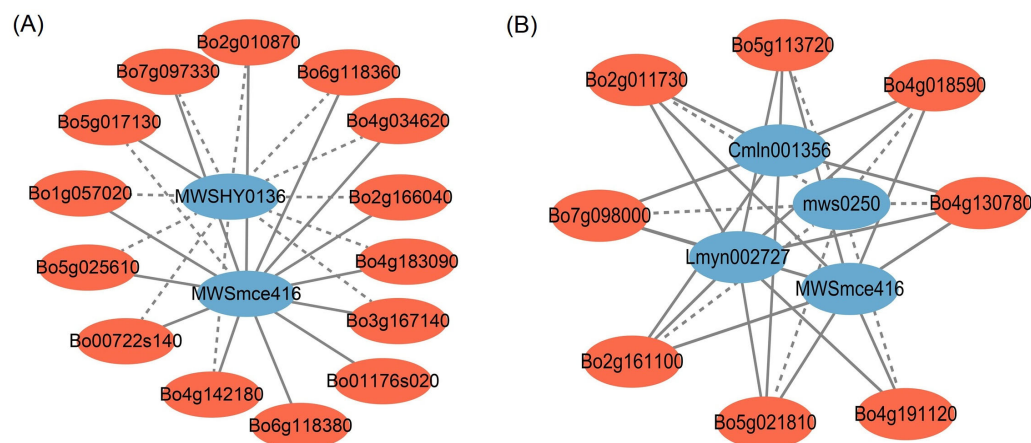

Figure 7. Connection network between DEGs (red ovals) and DAMs (blue ovals) of glucoraphanin biosynthesis in stalk (**A**) and floret (**B**). Blue and red ovals represent metabolites and genes, respectively. Solid line represents positive correlation, and dash line represents negative correlation.

4. Discussion

4.1. DEGs Related to Glucoraphanin Biosynthesis in Different Organs

Glucoraphanin is a major GSL in broccoli [25]. Previous studies have shown that *BCAT* and *MAM* are crucial enzymes in deamination and transamination during side chain extension [27–29]. In this study, we found that *BCAT2* was differentially expressed in the stalk, and *BCAT4*, *MAM1/2* in the leaf and floret (Figure 2D–F). The upregulated expression of them is an important factor in glucoraphanin accumulation [33]. For the formation of core structure, *CYP*, *GST*, *UGT*, *SOT* family genes played a crucial role in a series of biochemical reactions [5,6]. In our study, *CYP79F1* was differentially expressed in all three plant parts, while *CYP83A1* was only differentially expressed in stalk (Figure 8). Moreover, we also detected some *GST* or novel homologous (*GSTF2*, *GSTF3*, *GSTT3* and *GSTU*) and *SOT* (*SOT15*, *SOT17* and *SOT18*) genes in different organs (Figure 8). Previous studies have shown that the accumulation of *FMOGS-OX* catalyzed the conversion of glucoerucin into glucoraphanin [34]. In this study, we also found that *FMOGS-OX2* and a homologous gene *FMOGS-OXL8* were differentially expressed in stalk and leaf, respectively (Table S6). Thus, the expression of these DEGs related to glucoraphanin was tissue and spatiotemporal-specific (Figure 8). This explained the different levels of glucoraphanin in different organs. In addition, we also found some novel homologous genes to functional genes, which participated in the process of conjugation of the activated aldoximes to a sulfur donor, and the conversion from S-oxygenated to aliphatic glucosinolates.
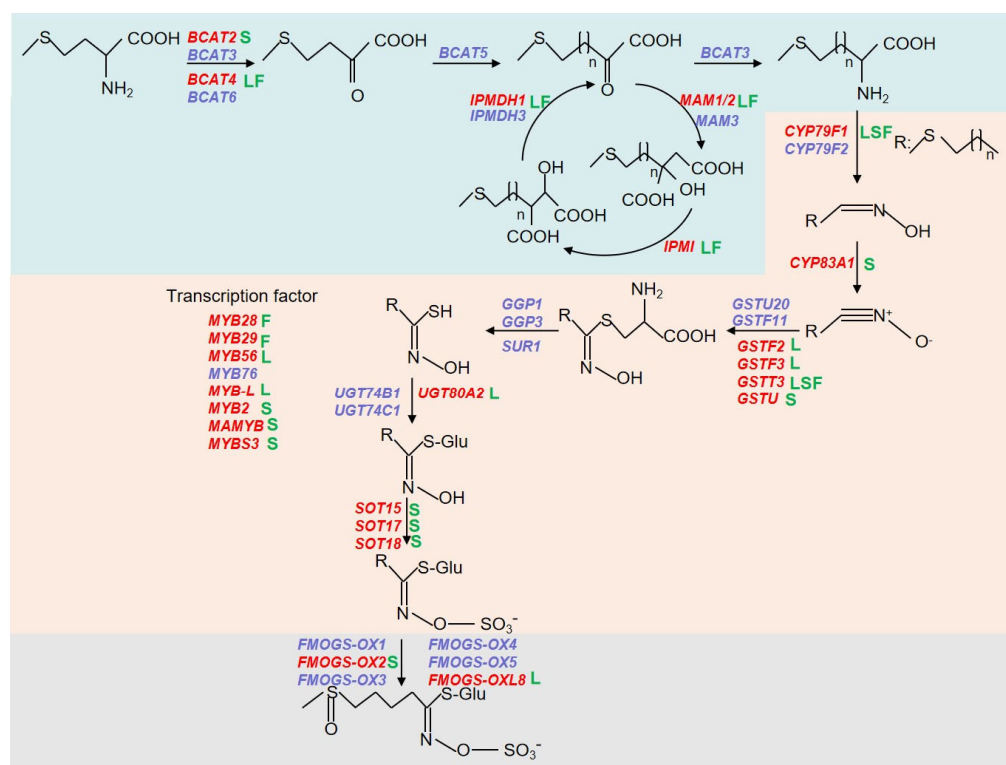
Figure 8. Schematic biosynthetic pathway of aliphatic glucosinolates and involved genes. Different background colors represent chain elongation machinery, biosynthesis of core glucosinolate structure and secondary modifications from top to bottom. Genes named in red were analyzed in this study. The green uppercase letters L, S, F behind the gene represent DEGs obtained in leaf, stalk and floret, respectively.

4.2. Effect of Glucosinolates Level on Plant Hormone Signal Transduction

It is well appreciated that plant hormones are crucial for the biosynthesis of glucosinolate and appropriate concentrations of plant hormones that result in the accumulation of GSLs in cruciferous vegetables [35–37]. Previous studies have shown that the accumulation of glucobrassicin and total GSLs increased in the broccoli (*B. oleracea* L. var. *italica*) suspension cultured cells after jasmonic acid (JA) treatment. Moreover, JA significantly increased the accumulation of total aliphatic GSLs and glucobrassicin in broccoli (*B. oleracea* L. var. *italica*) sprouts [38]. It has been reported that after the methyl jasmonate (MeJA) treatment, the content of total GSLs, glucobrassicin, gluconasturtiin and neoglucobrassicin in the floret and flower bulb increased in broccoli (*B. oleracea* L. var. *italica*) [39,40]. In this study, we found some DEGs related to JA and MeJA between the high and low RAA content pools. Among them, *TIF7* and *TIF9* were upregulated in the high RAA content pool of stalk, and *TIF10* was upregulated in the high RAA content pool of floret (Table S10). They belong to the *TIFY* family, which plays a crucial role in cross-talk between Jasmonic acid and other phytohormones pathways [41]. Moreover, *JAR1*, which encodes a jasmonate-amido synthetase, was upregulated in the high RAA content pool of stalk (Table S10).

Appropriate concentrations of auxins such as indole-3-acetic acid (IAA), indolebutyric acid (IBA) and naphthylacetic acid (NAA) increase the accumulation of glucosinolates. Studies have shown that 0.1 mg/L IAA, IBA and NAA treatment increase the accumulation of glucoraphanin, gluconapin, glucoerucin, glucobrassicin, gluconasturtiin, and indolic GSLs in the broccoli (*Brassica oleracea* L. var. *capitata* L.) hairy root, respectively [42]. In our study, we also identified some DEGs related to auxins. Among them, *IAA5*, *IAA29*, *IAA30*, *IAA32*, *GH3-2*, *GH3-3* and *SAU20* were upregulated in the high RAA content pool of stalk, *IAA7* and *SAU50* were upregulated in the high RAA content pool of floret (Table S10). *IAA*, *GH3* and *SAU* families, which belong to early auxin-responsive genes, are

specifically induced by auxin within minutes [43,44]. Therefore, plant hormones increase the accumulation of glucosinolates; in turn, the glucosinolate levels also upregulated the expression of phytohormone-related genes.

4.3. Effect of Glucosinolates Level on Flavonoids

Different secondary metabolites not only have unique biosynthetic pathways, but also crosstalk with each other to regulate plant growth and adapt to environmental changes [45]. Flavonoids are a group of secondary metabolites that are known to have beneficial health effects in humans and other animals [46]. Multiple flavonoids were tentatively suggested in the broccoli extracts from comparison with a general metabolomics database. Some of them had previously been conclusively demonstrated from the species *B. oleraceae* (Table S11). Flavonoids biosynthesis occurs primarily in the cytoplasm and endoplasmic reticulum, and its synthetic pathway is initiated by chalcones, one of the products of the phenylpropanoid biosynthesis pathway [47]. Studies have shown that the accumulation of some aldoxime (among the precursors of glucosinolates) limits phenylpropanoid production [45,48]. Therefore, we speculate that the restriction of aldoxime on phenylpropanoid synthesis would be released when the glucosinolate synthesis is increased, and it would indirectly promote the production of flavonoids. In our study, metabolite analysis results showed that compared with the low RAA content pool, the content of most of the tentatively suggested flavonoids was upregulated in the high RAA content pool of stalks and florets (Table S11). In addition, we found some DEGs related to flavonoid biosynthesis were upregulated between the high and low RAA content in stalks and florets (Table S12). Among them, flavonol synthase (*FLS*), Cytochrome P450C4H (*P450C4H*) and Cytochrome P450 75B1 (*CYP75B1*) play a crucial role in the flavonoids biosynthesis pathway [47,49]. This observation would also suggest crosstalk between glucosinolates biosynthesis and flavonoids biosynthesis pathways.

5. Conclusions

To analyze the differences of genes related to glucosinolate biosynthesis in different plant parts of broccoli, we selected extreme individuals from an F_2 population of broccoli and mixed them to form low and high glucoraphanin content pools of leaf, stalk and floret, respectively. The combination of transcriptome and metabolome analysis revealed that some genes such as *Bo5g113720*, *Bo2g161100* and *Bo7g09800*, *Bo4g018590*, *Bo5g021810*, and *Bo2g011730* showed different expression trends between low and high glucoraphanin content pools, which increased the accumulation of glucoraphanin. These genes have different expression levels in the three plant parts. Notably, the accumulation of glucoraphanin upregulated the expression of plant hormone signal transduction-related genes, such as *TIFY*, *JAR1*, *IAA*, *GH3* and *SAU*. In addition, the accumulation of glucoraphanin also increased the levels of flavonoid metabolites. Thus, our study deepens the understanding of glucosinolate biosynthesis at the molecular level, and also provides evidence for the crosstalk between the glucosinolates and flavonoids biosynthesis pathways.

Supplementary Materials: The following supporting information can be downloaded at: https://www.mdpi.com/article/10.3390/app13105837/s1, Figure S1. The glucosinolates content of parents and their F2 population. (A) Comparison of glucosinolates content between B0401 and MS84003 at commercial stage. RAA, (RS)-4-(methylsulfinyl)butyl GSL (Glucoraphanin), GBC, Indol-3-methyl GSL (Glucobrassicin), ERU, 4-(Methylsulfanyl)butyl GSL (Glucoerucin), ALY, (RS)-5-(Methylsulfinyl)pentyl GSL (Glucoalyssin), 4ME, 4-Methoxyindol-3-ylmethyl GSL (4-methoxyglucobrassicin), NEO, 1-Methoxyindol-3-ylmethyl GSL (Neoglucobrassicin). *** $p < 0.01$. Frequency histogram of RAA in leaf (B), stalk (C) at vegetative growth stage and floret (D) at commercial stage in F2 plants. FW, fresh weight; DW, dry weight. Figure S2. The number of transcripts annotated by KEGG, nonredundant (NR), Swiss-Prot, EuKaryotic Orthologous Groups (KOG), GO and Pfam databases. LTL, STL and FTL represent low RAA content pools in leaf, stalk and floret, respectively. LTH, STH and FTH represent high RAA content pools in leaf, stalk and floret, respectively. Figure S3. GO classification analysis of differential expression genes. (A) LTL vs. LTH, (B) STL vs. STH, (C)

FTL vs. FTH. LTL, STL and FTL represent low RAA content pools in leaf, stalk and floret, respectively. LTH, STH and FTH represent high RAA content pools in leaf, stalk and floret, respectively. Figure S4. Phylogenetic analysis of DEGs involved in glucosinolate biosynthesis. Phylogenetic tree of *Bo5g113720* (A), *Bo2g011730* (B), *Bo2g161100* and *Bo7g098000* (C), *Bo4g018590* (D), *Bo5g02181* (E) and *Bo6g083740* (F). Mega 7.0 was used to build the phylogenetic tree by the neighbor-joining method (https://www.megasoftware.net/, accessed on 25 August 2022). The scale bar indicates a branch length of 0.1. Red and blue boxes represent the gene itself and genes with functional annotations in *Brassica rapa* and *Arabidopsis thaliana*. Figure S5. PCA of differentially accumulated metabolites in LML vs. LMH (A), SML vs. SMH (B), and FML vs. FMH (C). LML, SML and FML represent low RAA content pools in leaf, stalk and floret, respectively. LMH, SMH and FMH represent high RAA content pools in leaf, stalk and floret, respectively. Figure S6. Coregulation among DAMs in all comparison groups. LML, SML and FML represent low RAA content pools in leaf, stalk and floret, respectively. LMH, SMH and FMH represent high RAA content pools in leaf, stalk and floret, respectively. Figure S7. Kyoto Encyclopedia of Genes and Genomes (KEGG) functional classification of differential accumulated metabolites (DAMs) in LML vs. LMH (A), SML vs. SMH (B), and FML vs. FMH (C) pools. The *X*-axis is the number of annotated genes to different categories of KEGG. The *Y*-axis represents different categories of KEGG. Blue column, Metabolism systems; Brown column, Environmental information processing. LML, SML and FML represent low RAA content pools in leaf, stalk and floret, respectively. LMH, SMH and FMH represent high RAA content pools in leaf, stalk and floret, respectively. Figure S8. KEGG pathway of DAMs in LML vs. LMH (A), SML vs. SMH (B), and FML vs. FMH (C) pools. The *X*-axis is the rich factor; the *Y*-axis represents the name of the pathway. The bubble size represents the number of DAMs involved. The bubble color indicates the enrichment degree of pathway and the size represents the number of DAMs enrichment in the pathway. LML, SML and FML represent low RAA content pools in leaf, stalk and floret, respectively. LMH, SMH and FMH represent high RAA content pools in leaf, stalk and floret, respectively. Figure S9. Correlation analysis between transcriptome and metabolome in LML vs. LMH and SML vs. SMH. The nine-quadrant diagram shows the correlation of genes and compounds between LML and LMH (A), SML and SMH (B). KEGG enrichment analysis of DEGs (red column) and DAMs (blue column) enriched in the same pathway in LML vs. LMH (C), SML vs. SMH (D). LML and SML represent low RAA content pools in leaf and stalk, respectively. LMH and SMH represent high RAA content pools in leaf and stalk, respectively. Table S1. Types and contents of glucosinolates in the two parental lines. Table S2. Sequencing, assembly statistics and comparative efficiency statistics for the 3 pairs transcriptomes of leaf, stalk and floret, respectively. Table S3. Summary of the DEGs and DAMs among 3 library pairs. Table S4. Twenty co-regulated DEGs statistics. Table S5. The top ten GO pathways of DEGs enrichment degree. Table S6. Differentially expressed genes related to glucosinolates synthesis process between low and high pools. Table S7. Primer sequences used in qRT-PCR analysis. Table S8. Categories of the metabolites identified in leaf, stalk and floret of F2 plants, respectively. Table S9. Co-regulated differential metabolites in leaf, stalk and floret. Table S10. DEGs related to plant hormone signal transduction between high and low RAA content. Table S11. DAMs related to flavonoids between high and low RAA content. Table S12. DEGs related to flavonoid biosynthesis between high and low RAA content. References [50–52] are listed in Table S11.

Data Availability Statement: The datasets presented in this study can be found in the Genome Sequence Archive in BIG Data Center (https://bigd.big.ac.cn/, accessed on 25 November 2022), Beijing Institute of Genomics (BIG), Chinese Academy of Sciences, under the accession number: CRA00927.

Conflicts of Interest: The authors declare no conflict of interest.

References

1. Vallejo, F.; Garcia-viguera, C.; Tomas-barberan, F.A. Changes in broccoli (*Brassica oleracea* var. italica) health-promoting compounds with inflorescence development. *J. Agric. Food Chem.* **2003**, *51*, 3776–3782. [CrossRef] [PubMed]
2. Fahey, J.W.; Zhang, Y.; Talalay, P. Broccoli sprouts: An exceptionally rich source of inducers of enzymes that protect against chemical carcinogens. *Proc. Natl. Acad. Sci. USA* **1997**, *94*, 10367–10372. [CrossRef] [PubMed]
3. Keck, A.S.; Qiao, Q.; Jeffery, E.H. Food matrix effects on bioactivity of broccoli-derived sulforaphane in liver and colon of f344 rats. *J. Agric. Food Chem.* **2003**, *51*, 3320–3327. [CrossRef] [PubMed]
4. Spitz, M.R.; Duphorne, C.M.; Detry, M.A.; Pillow, P.C.; Amos, C.I.; Lei, L.; de Andrade, M.; Gu, X.; Hong, W.K.; Wu, X. Dietary intake of isothiocyanates: Evidence of a joint effect with glutathione S-transferase polymorphisms in lung cancer risk. *Cancer Epidemiol. Biomarkers Prev.* **2000**, *9*, 1017–1020.
5. Sonderby, I.E.; Geu-Flores, F.; Halkier, B.A. Biosynthesis of glucosinolates–gene discovery and beyond. *Trends Plant Sci.* **2010**, *15*, 283–290. [CrossRef]
6. Wang, H.; Wu, J.; Sun, S.L.; Liu, B.; Cheng, F.; Sun, R.F.; Wang, X.W. Glucosinolate biosynthetic genes in *Brassica rapa*. *Gene* **2011**, *487*, 135–142. [CrossRef]
7. Prieto, M.A.; Lopez, C.J.; Simal-Gandara, J. Glucosinolates: Molecular structure, breakdown, genetic, bioavailability, properties and healthy and adverse effects. *Adv. Food Nutr. Res.* **2019**, *90*, 305–350.
8. Connolly, E.L.; Sim, M.; Travica, N.; Marx, W.; Beasy, G.; Lynch, G.S.; Bondonno, C.P.; Lewis, J.R.; Hodgson, J.M.; Blekkenhorst, L.C. Glucosinolates from cruciferous vegetables and their potential role in chronic disease: Investigating the preclinical and clinical evidence. *Front. Pharmacol.* **2021**, *12*, 767975. [CrossRef]
9. Abdull Razis, A.F.; De Nicola, G.R.; Pagnotta, E.; Iori, R.; Ioannides, C. 4-Methylsulfanyl-3-butenyl isothiocyanate derived from glucoraphasatin is a potent inducer of rat hepatic phase II enzymes and a potential chemopreventive agent. *Arch. Toxicol.* **2012**, *86*, 183–194. [CrossRef]
10. Lee, Y.R.; Chen, M.; Lee, J.D.; Zhang, J.; Lin, S.Y.; Fu, T.M.; Chen, H.; Ishikawa, T.; Chiang, S.Y.; Katon, J.; et al. Reactivation of *PTEN* tumor suppressor for cancer treatment through inhibition of a MYC-WWP1 inhibitory pathway. *Science* **2019**, *364*, e0159. [CrossRef]
11. Rangkadilok, N.; Tomkins, B.; Nicolas, M.E.; Premier, R.R.; Bennett, R.N.; Eagling, D.R.; Taylor, P.W. The effect of post-harvest and packaging treatments on glucoraphanin concentration in broccoli (*Brassica oleracea* var. italica). *J. Agric. Food Chem.* **2002**, *50*, 7386–7391. [CrossRef] [PubMed]
12. Lim, Y.P.; Li, Z.S.; Liu, Y.M.; Li, L.Y.; Fang, Z.Y.; Yang, L.M.; Zhuang, M.; Zhang, Y.Y.; Lv, H.H. Transcriptome reveals the gene expression patterns of sulforaphane metabolism in broccoli florets. *PLoS ONE* **2019**, *14*, e0213902.
13. Fahey, J.W.; Holtzclaw, W.D.; Wehage, S.L.; Wade, K.L.; Stephenson, K.K.; Talalay, P. Sulforaphane bioavailability from glucoraphanin-rich broccoli: Control by active endogenous myrosinase. *PLoS ONE* **2015**, *10*, e0140963. [CrossRef] [PubMed]
14. Vanduchova, A.; Anzenbacher, P.; Anzenbacherova, E. Isothiocyanate from broccoli, sulforaphane, and its properties. *J. Med. Food* **2019**, *22*, 121–126. [CrossRef]
15. Jiang, X.; Liu, Y.; Ma, L.X.; Ji, R.; Qu, Y.Q.; Xin, Y.; Lv, G.Y. Chemopreventive activity of sulforaphane. *Drug Des. Devel. Ther.* **2018**, *12*, 2905–2913. [CrossRef]
16. Kim, J.K.; Park, S.U. Current potential health benefits of sulforaphane. *EXCLI J.* **2016**, *15*, 571–577.
17. Bai, Y.; Wang, X.L.; Zhao, S.; Ma, C.Y.; Cui, J.W.; Zheng, Y. Sulforaphane protects against cardiovascular disease via *Nrf2* activation. *Oxid. Med. Cell. Longev.* **2015**, *2015*, 407580. [CrossRef]
18. Blaževi'c, I.; Montaut, S.; Burčul, F.; Olsen, C.E.; Burow, M.; Rollin, P.; Agerbirk, N. Glucosinolate structural diversity, identification, chemical synthesis and metabolism in plants. *Phytochemistry* **2020**, *169*, 112100. [CrossRef]
19. Halkier, B.A.; Gershenzon, J. Biology and biochemistry of glucosinolates. *Annu. Rev. Plant Biol.* **2006**, *57*, 303–333. [CrossRef]
20. Agerbirk, N.; Olsen, C.E. Glucosinolate structures in evolution. *Phytochemistry* **2012**, *77*, 16–45. [CrossRef]
21. Zhang, C.L.; Di, H.M.; Lin, P.X.; Wang, Y.T.; Li, Z.Q.; Lai, Y.S.; Li, H.X.; Sun, B.; Zhang, F. Genotypic variation of glucosinolates and their breakdown products in mustard (*Brassica juncea*) seeds. *Sci. Hortic.* **2022**, *294*, 110765. [CrossRef]
22. Jung, S.J.; Shiva, R.B.; Gwan, H.K.; Jun, G.L. Yearly variation in glucosinolate content in inflorescences of broccoli breeding lines. *Korean J. Hortic. Sci.* **2018**, *36*, 406–416.
23. Rybarczyk-Plonska, A.; Hagen, S.F.; Borge, G.I.A.; Bengtsson, G.B.; Hansen, M.K.; Wold, A.B. Glucosinolates in broccoli (*Brassica oleracea* L. var. italica) as affected by postharvest temperature and radiation treatments. *Postharvest Biol. Technol.* **2016**, *116*, 16–25. [CrossRef]
24. Charron, C.S.; Saxton, A.M.; Sams, C.E. Relationship of climate and genotype to seasonal variation in the glucosinolate-myrosinase system. I. glucosinolate content in ten cultivars ofBrassica oleracea grown in fall and spring seasons. *J. Sci. Food Agric.* **2005**, *85*, 671–681. [CrossRef]

25. Guo, L.P.; Yang, R.Q.; Wang, Z.Y.; Guo, Q.H.; Gu, Z.X. Glucoraphanin, sulforaphane and myrosinase activity in germinating broccoli sprouts as affected by growth temperature and plant organs. *J. Funct. Foods* **2014**, *9*, 70–77. [CrossRef]

26. Brader, G.; Mikkelsen, M.D.; Halkier, B.A.; Tapio Palva, E. Altering glucosinolate profiles modulates disease resistance in plants. *Plant J.* **2006**, *46*, 758–767. [CrossRef]

27. Wittstock, U.; Halkier, B.A. Glucosinolate research in the *Arabidopsis* era. *Trends Plant Sci.* **2002**, *7*, 263–270. [CrossRef]

28. Tian, P.; Lu, X.; Bao, J.Y.; Zhang, X.M.; Lu, Y.Q.; Zhang, X.L.; Wei, Y.C.; Yang, J.; Li, S.; Ma, S.Y. Transcriptomics analysis of genes induced by melatonin related to glucosinolates synthesis in broccoli hairy roots. *Plant Signal. Behav.* **2021**, *16*, 1952742. [CrossRef]

29. Grubb, C.D.; Abel, S. Glucosinolate metabolism and its control. *Trends Plant Sci.* **2006**, *11*, 89–100. [CrossRef]

30. Seo, M.S.; Kim, J.S. Understanding of *MYB* transcription factors involved in glucosinolate biosynthesis in *Brassicaceae*. *Molecules* **2017**, *22*, 1549. [CrossRef]

31. Yu, X.L.; He, H.J.; Zhao, X.Z.; Liu, G.M.; Hu, L.P.; Cheng, B.; Wang, Y.Q. Determination of 18 intact glucosinolates in *Brassicaceae* vegetables by UHPLC-MS/MS: Comparing tissue disruption methods for sample preparation. *Molecules* **2021**, *27*, 231. [CrossRef]

32. Schmittgen, T.D.; Livak, K.J. Analyzing real-time PCR data by the comparative CT method. *Nat. Protoc.* **2008**, *3*, 1101–1108. [CrossRef]

33. Yin, L.; Chen, C.M.; Chen, G.J.; Cao, B.H.; Lei, J.J. Molecular Cloning, Expression Pattern and Genotypic Effects on Glucoraphanin Biosynthetic Related Genes in Chinese Kale (*Brassica oleracea* var. alboglabra Bailey). *Molecules* **2015**, *20*, 20254–20267. [CrossRef]

34. Li, J.; Hansen, B.G.; Ober, J.A.; Kliebenstein, D.J.; Halkier, B.A. Subclade of flavin-monooxygenases involved in aliphatic glucosinolate biosynthesis. *Plant Physiol.* **2008**, *148*, 1721–1733. [CrossRef]

35. Traw, M.B.; Kim, J.; Enright, S.; Ciollini, D.F.; Bergelson, J. Negative cross-talk between salicylate- and jasmonate-mediated pathways in the assilewskija ecotype of *Arabidopsis thaliana*. *Mol. Ecol.* **2003**, *12*, 1125–1135. [CrossRef]

36. Fritz, V.A.; Justen, V.L.; Bode, A.M.; Schuster, T.; Wang, M. Glucosinolate enhancement in cabbage induced by jasmonic acid application. *HortScience* **2010**, *45*, 1188–1191. [CrossRef]

37. Liu, Z.C.; Wang, H.P.; Lv, J.; Luo, S.L.; Hu, L.L.; Wang, J.; Li, L.S.; Zhang, G.B.; Xie, J.M.; Yu, J.H. Effects of plant hormones, metal ions, salinity, sugar, and chemicals pollution on glucosinolate biosynthesis in cruciferous Plant. *Front. Plant Sci.* **2022**, *13*, 856442. [CrossRef]

38. Kastell, A.; Smetanska, I.; Ulrichs, C.; Cai, Z.; Mewis, I. Effects of phytohormones and jasmonic acid on glucosinolate content in hairy root cultures of *Sinapis alba* and *Brassica rapa*. *Appl. Biochem. Biotechnol.* **2013**, *169*, 624–635. [CrossRef]

39. Chiu, Y.C.; Matak, K.; Ku, K.M. Methyl jasmonate treated broccoli: Impact on the production of glucosinolates and consumer preferences. *Food Chem.* **2019**, *299*, 125099. [CrossRef]

40. Ku, K.M.; Becker, T.; Juvik, J. Transcriptome and metabolome analyses of glucosinolates in two broccoli cultivars following jasmonate treatment for the induction of glucosinolate defense to *Trichoplusia ni* (Hübner). *Int. J. Mol. Sci.* **2016**, *17*, 1135. [CrossRef]

41. Singh, P.; Mukhopadhyay, K. Comprehensive molecular dissection of *TIFY* Transcription factors reveal their dynamic responses to biotic and abiotic stress in wheat (*Triticum aestivum* L.). *Sci. Rep.* **2021**, *11*, 9739. [CrossRef]

42. Kim, H.H.; Kwon, D.Y.; Bae, H.H.; Kim, S.J.; Kim, Y.B.; Uddin, M.D.R.; Park, S.U. Influence of auxins on glucosinolate biosynthesis in hairy root cultures of broccoli (*Brassica oleracea* var. italica). *Asian J. Chem.* **2013**, *25*, 6099–6101. [CrossRef]

43. Hagen, G.; Guilfoyle, T. Auxin-responsive gene expression: Genes, promoters and regulatory factors. *Plant Mol. Biol.* **2002**, *49*, 373–385. [CrossRef]

44. Liscum, E.; Reed, J.W. Genetics of Aux/IAA and ARF action in plant growth and development. *Plant Mol. Biol.* **2002**, *49*, 387–400. [CrossRef]

45. Kim, J.I.; Zhang, X.; Pascuzzi, P.E.; Liu, C.J.; Chapple, C. Glucosinolate and phenylpropanoid biosynthesis are linked by proteasome-dependent degradation of *PAL*. *New Phytol.* **2020**, *225*, 154–168. [CrossRef]

46. Saito, K.; Yonekura-Sakakibara, K.; Nakabayashi, R.; Higashi, Y.; Yamazaki, M.; Tohge, T.; Fernie, A.R. The flavonoid biosynthetic pathway in Arabidopsis: Structural and genetic diversity. *Plant Physiol. Biochem.* **2013**, *72*, 21–34. [CrossRef]

47. Bell, L.; Oruna-Concha, M.J.; Wagstaff, C. Identification and quantification of glucosinolate and flavonol compounds in rocket salad (*Eruca sativa*, *Eruca vesicaria* and *Diplotaxis tenuifolia*) by LC-MS: Highlighting the potential for improving nutritional value of rocket crops. *Food Chem.* **2015**, *172*, 852–861. [CrossRef]

48. Mach, J. Metabolic crosstalk: Interactions between the phenylpropanoid and glucosinolate pathways in *Arabidopsis*. *Plant Cell* **2015**, *27*, 1367. [CrossRef]

49. Tan, B.A.; Daim, L.D.J.; Ithnin, N.; Ooi, T.E.K.; Md-Noh, N.; Mohamed, M.; Mohd-Yusof, H.; Appleton, D.R.; Kulaveerasingam, H. Expression of phenylpropanoid and flavonoid pathway genes in oil palm roots during infection by Ganoderma boninense. *Plant Gene* **2016**, *7*, 11–20. [CrossRef]

50. Cartea, M.E.; Francisco, M.; Soengas, P.; Velasco, P. Phenolic Compounds in Brassica Vegetables. *Molecules* **2011**, *16*, 251–280. [CrossRef]

51. Schmidt, S.; Zietz, M.; Schreiner, M.; Rohn, S.; Kroh, L.W.; Krumbein, A. Identification of complex, naturally occurring flavonoid glycosides in kale (*Brassica oleracea* var. sabellica) by high-performance liquid chromatography diode-array detection/electrospray ionization multi-stage mass spectrometry. *Rapid Commun. Mass Spectrom.* **2010**, *24*, 2009–2022. [CrossRef]
52. Vallejo, F.; Tomás-Barberán, F.A.; Ferreres, F. Characterisation of flavonols in broccoli (*Brassica oleracea* L. var. italica) by liquid chromatography-uV diode-array detection-electrospray ionisation mass spectrometry. *J. Chromatogr. A* **2004**, *1054*, 181–193. [CrossRef]